

## Graphical Abstract

### **Electronic and magnetic properties of graphene quantum dots with two charged vacancies**

E. Bulut Kul, M. Polat, A. D. Güçlü

arXiv:2006.11048v2 [cond-mat.mes-hall] 20 Aug 2020

## Highlights

### **Electronic and magnetic properties of graphene quantum dots with two charged vacancies**

E. Bulut Kul, M. Polat, A. D. Güçlü

- Investigation of electron-electron interaction effects in frustrated collapse in graphene systems
- Emergence of non-magnetic regime within the subcritical collapse region.
- Renormalization of frustrated critical coupling constant  $\beta_{cf}$ .

# Electronic and magnetic properties of graphene quantum dots with two charged vacancies

E. Bulut Kul\*, M. Polat (Researcher) and A. D. Güçlü (Co-ordinator)

Department of Physics, Izmir Institute of Technology, IZTECH, TR35430, Izmir, Turkey

## ARTICLE INFO

### Keywords:

Graphene nanostructures

Magnetization

Atomic collapse

Vacancy

## ABSTRACT

Electronic and magnetic properties of a system of two charged vacancies in hexagonal shaped graphene quantum dots are investigated using a mean-field Hubbard model as a function of the Coulomb potential strength  $\beta$  of the charge impurities and the distance  $R$  between them. For  $\beta = 0$ , the magnetic properties of the vacancies are dictated by Lieb's rules where the opposite (same) sublattice vacancies are coupled antiferromagnetically (ferromagnetically) and exhibit Fermi oscillations. Here, we demonstrate the emergence of a non-magnetic regime within the subcritical region: as the Coulomb potential strength is increased to  $\beta \sim 0.1$ , before reaching the frustrated atomic collapse regime, the magnetization is strongly suppressed and the ground state total spin projection is given by  $S_z = 0$  both for opposite and same sublattice vacancy configurations. When long-range electron-electron interactions are included within extended mean-field Hubbard model, the critical value for the frustrated collapse increases from  $\beta_{cf} \sim 0.28$  to  $\beta_{cf} \sim 0.36$  for  $R < 27 \text{ \AA}$ .

## 1. Introduction


Recent advances at the atomic scale control of graphene through vacancies [1–4], charged impurities [5, 6] and adatoms [7–11] open up possibilities for tailoring graphene's electronic and magnetic properties [12–17] for future spintronic and computing applications, as well as for investigating relativistic quantum effects such as atomic collapse [6, 18–23]. While pure graphene is not expected to be magnetic, breaking of the sublattice symmetry of the honeycomb lattice through atomic defects is expected to exhibit local magnetization as predicted by theoretical calculations [12, 24–29]. This local magnetization was recently observed experimentally using scanning tunneling microscopy (STM) around hydrogen adatoms [30] and single atomic vacancies [4].

On the other hand, Mao et al. [31] have shown that carbon vacancies in graphene can host a stable positive effective charge  $Z$  which can be gradually increased by applying STM voltage pulses. This tunability of the coupling constant  $\beta = Z\alpha_g$ , where  $\alpha_g = 2.2/\kappa$  is the effective fine-structure constant and  $\kappa$  is the dielectric constant, allows the observation of the system to undergo a transition from subcritical to supercritical regime where the 1S-like state dives into Dirac continuum, forming quasi-bound states and mimicking the atomic collapse expected to occur in ultra-heavy nuclei [32–37] with  $Z \sim 172$  [38] which do not exist in nature. Theoretically predicted by Pereira et al. [39], the atomic collapse in graphene was first successfully observed through clusters of charged calcium dimers [6]. On the other hand, when two or more impurities with identical charges are present a frustrated supercritical regime occurs at a distance dependent critical value  $\beta_{cf}$  which is lower than the critical value  $\beta_c = 0.5$  for a single charge impurity [23, 40, 41].

An open question that we address in this work is, how do charged vacancies magnetically couple to each other as a function of  $\beta$ . For  $\beta = 0$ , a theorem due to Lieb for bipartite Hubbard systems predicts [42] that the local magnetic moments formed around the vacancies should couple to each other ferromagnetically or antiferromagnetically over large distances depending on whether they lie on the same or opposite sublattices. Moreover, as the system is reminiscent of Ruderman-Kittel-Kasuya-Yoshida (RKKY) model, one expects to observe oscillations of magnetic coupling if the vacancies are along the zigzag directions as opposed to a smooth decrease along the armchair directions [43]. On the other hand, as  $\beta$  is increased, Lieb's theorem does not apply anymore, the local magnetization around vacancies is suppressed and one expects the magnetic coupling between the two local moments to be severely distorted.

In this work, we consider a finite size graphene quantum dot (GQD) [43–50] with hexagonal armchair edges to investigate the magnetic coupling properties between the charged vacancies. The armchair edges make the system free of additional edge state effects. Moreover, the critical  $\beta$  value for which the 1S state crosses the Dirac point is known to be independent of the size of the quantum dot both within effective mass approximation and mean-field Hubbard models [51, 52]. Thus, the hexagonal GQD system provides us with a practical way to understand bulk properties as well. Here, we perform mean-field Hubbard calculations to show that the magnetization of the vacancies is strongly suppressed for  $\beta > 0.1$  which is in the subcritical regime, i.e., lower than the frustrated critical value  $\beta_{cf} \sim 0.28$  for the range of  $R$  studied here. As a result, the ground state total spin projection of the double vacancy system reduces to  $S_z = 0$  for both opposite (AB) and same (AA) sublattice configurations. When we include long-range electron-electron interactions within extended MFH approximation,  $\beta_{cf}$  is renormalized from 0.28 to 0.36 by suppression of overscreening [24, 53, 54]. We also investigated the effect of second nearest neighbor hop-

\*Corresponding author

 bulutkul@iyte.edu.tr (E.B. Kul)

ORCID(s): 0000-0003-2392-4313 (E.B. Kul); 0000-0002-1372-1945 (M. Polat); 0000-0002-4351-7216 (A.D. Güçlü)

ping  $t_{nm}$ . For  $t_{nm} = 0.2$  eV, we found that Lieb's predictions for magnetization of same sublattice vacancy system is violated even for  $\beta = 0$ .

## 2. Model and Method

We use a one-band mean-field Hubbard (MFH) model where the single electrons states are written as a linear combination of  $p_z$  orbitals on every carbon atom since the sigma orbitals are considered to be mainly responsible for mechanical stability of graphene. Including long range interactions, the extended mean-field Hubbard Hamiltonian can be written as

$$\begin{aligned}
 H_{MFH} = & \sum_{ij\sigma} t_{ij}(c_{i\sigma}^\dagger c_{j\sigma} + h.c.) \\
 & + U \sum_{i\sigma} (\langle n_{i\bar{\sigma}} \rangle - \frac{1}{2}) n_{i\sigma} \\
 & + \sum_{ij} V_{ij} (\langle n_j \rangle - 1) n_i \\
 & + \sum_{i\sigma} V_C(\mathbf{r}_i) c_{i\sigma}^\dagger c_{i\sigma}
 \end{aligned} \quad (1)$$

where the first term represents the tight-binding Hamiltonian and  $t_{ij}$ 's are the hopping parameters given by  $t_{nn} = -2.8$  eV for nearest neighbors and  $t_{nmn} = -0.1$  eV for next nearest-neighbors [14]. Additionally, in this work we considered  $t_{nmn} = 0$  eV and  $t_{nmn} = -0.2$  eV to investigate the stability of Lieb's theorem against  $t_{nmn}$ . The  $c_{i\sigma}^\dagger$  and  $c_{i\sigma}$  are creation and annihilation operators for an electron at the  $i$ -th orbital with spin  $\sigma$ , respectively. Expectation value of electron densities are represented by  $\langle n_{i\sigma} \rangle$ . The second term represents on-site Coulomb interactions. We take on-site interaction parameter as  $U = 16.522/\kappa$  eV, with effective dielectric constant  $\kappa = 6$  to take into account screening effects due to substrate [55]. The third term stands for long-range Coulomb interaction. Interaction parameters  $V_{ij} = 8.64/\kappa$  and  $V_{ij} = 5.33/\kappa$  for the first and next nearest neighbors respectively, numerically calculated using Slater  $p_z$  orbitals [56]. Beyond second nearest neighbors, interactions are calculated assuming point charges. Finally, the last term represents the Coulomb potential due to vacancy charges located at  $\mathbf{R}_1$  and  $\mathbf{R}_2$ , expressed as

$$V_C(\mathbf{r}_i) = -\hbar v_F \beta \left( \frac{1}{|\mathbf{r}_i - \mathbf{R}_1|} + \frac{1}{|\mathbf{r}_i - \mathbf{R}_2|} \right) \quad (2)$$

where  $v_F = 3at/2$  ( $\sim 10^6$  m/s) is the Fermi velocity. The dimensionless Coulomb potential strength  $\beta$  can be tuned as discussed above. In this work, we assume that the charged impurities cause ideal vacancies in the honeycomb lattice where relaxation and bond reconstruction effects are neglected.

The hexagonal armchair quantum dot system that we consider in this work consists of 5512 atoms for MFH calculations and up to 10806 atoms for TB calculations. A critical step in the numerical calculations is the initial guess state used for the self-consistent diagonalization of the MFH Hamiltonian. We have used various initial guess spin states

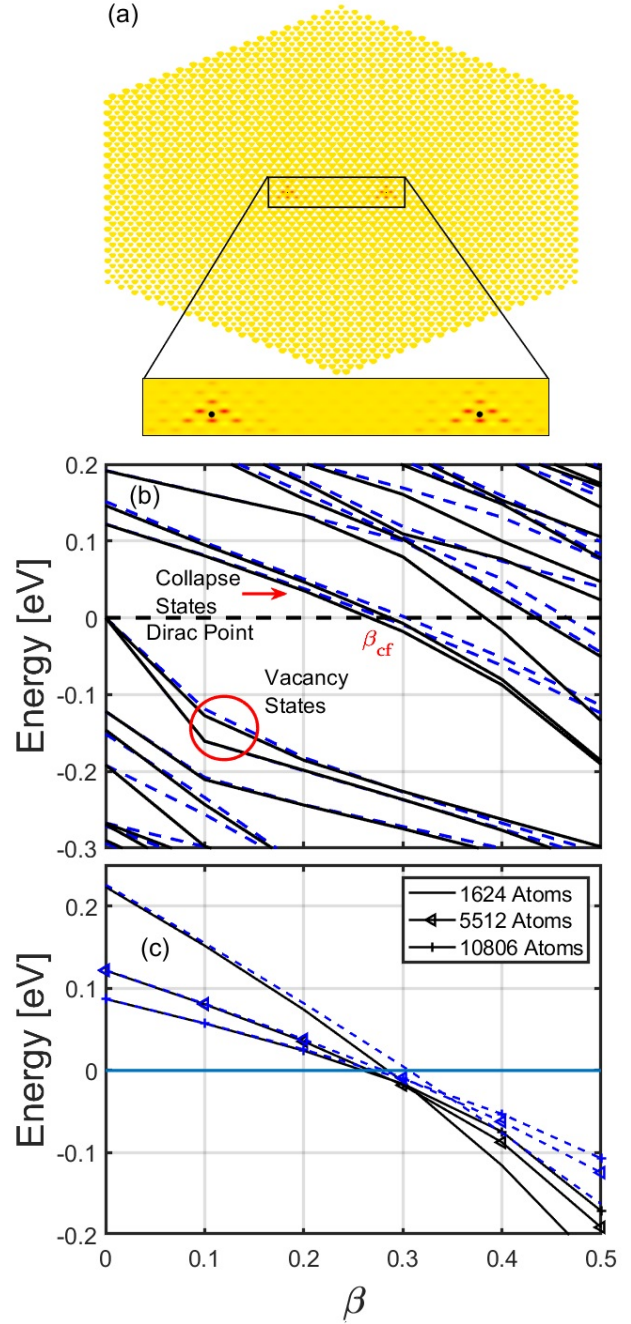


**Figure 1:** (a) Cross section image of electron density for a hexagonal armchair GQD, 5512 atoms, with two vacancies for AA case. Inter-vacancy distance is set to  $R = 11b$  where  $b$  is second nearest-neighbor distance. Black dots represent vacancy positions. (b) TB energy spectrum versus  $\beta$  and (c) GQD size comparison for  $R/b = 3$  (black-solid lines) and  $R/b = 9$  (blue-dashed lines).

to ensure to the convergence to lowest possible ground states consistent with the two competing total spin projections  $S_z = 1$  (ferromagnetic coupling) and  $S_z = 0$  (antiferromagnetic coupling).

### 3. Results and Discussion

#### 3.1. Tight-binding results

As mentioned above, we consider AA and AB configurations for vacancies located along the zigzag direction and separated by a distance  $R$ , as shown in Fig. 1a for the AA configuration. The midpoint between the vacancies is chosen to be the center of the dot to minimize edge effects. Fig. 1b shows a typical tight-binding (TB) energy spectrum as a function of  $\beta$  in the vicinity of the Dirac point, obtained for the AA configuration with  $R/b = 3$  (solid lines) and  $R/b = 9$  (dashed lines) where  $b = 2.46 \text{ \AA}$  is the second nearest neighbor distance. As expected, there are two sets of vacancy states and collapse states corresponds to the bonding and anti-bonding states [40, 41] of two charged vacancies. Collapsing states cross the Dirac level at the critical value  $\beta_{cf} \sim 0.28$  indicating the lower limit for the frustrated supercritical regime before the system enters the molecular collapse regime at  $\beta_c = 0.5$  [23, 40, 41]. The lower value of  $\beta_{cf} = 0.28$  for the double impurity system is expected since the Coulomb potential due to each impurity feed each other, accelerating the collapse. This effect is expected to vanish for large distances  $R$ . For the range of  $R$  values studies in this work,  $\beta_{cf}$  is nearly constant. More importantly,  $\beta_{cf}$  is also found to be largely independent of finite size effects for dots larger than few thousands atoms, consistent with single charged impurity results [51] as seen in Fig. 1c, provided  $R$  is smaller than the dot diameter. We also note that, increasing  $\beta$  lifts the degeneracy of the vacancy states initially. The energy gap between the vacancy states increases up to  $\beta \sim 0.1$  but, starts decreasing again as  $\beta$  is increased further, pointing to a decoupling of bonding and anti-bonding vacancy states at large  $\beta$  values. This observation have important consequences for the understanding of mean-field Hubbard results discussed below.

#### 3.2. Mean-Field Hubbard results for bare vacancies

In order to understand magnetic properties, we first focus on  $\beta = 0$  and examine the stability of magnetic coupling between the vacancies. Figure 2a and 2c show the spin gap  $E_{S_z=1} - E_{S_z=0}$  as a function of distance  $R$  for AA and AB configurations respectively, obtained using MFH (without long range interactions  $V_{ij}$ ) for different second nearest neighbor hopping parameters  $t_{nnn}$ . For  $t_{nnn} = 0$ , ferromagnetic ( $S_z = 1$ ) ground state for AA configuration and antiferromagnetic ( $S_z = 0$ ) ground state for AB configuration are obtained as expected. Moreover, the observed distance dependent oscillations are reminiscent of RKKY model for graphene along zigzag direction [43, 57], assuming  $E_{S_z=1} - E_{S_z=0}$  is proportional to the effective magnetic coupling parameter  $J$  in the RKKY model. Here, however, the spins are localized on three atoms neighboring each vacancy unlike in the RKKY model. We have also investigated (not shown) the behavior of  $E_{S_z=1} - E_{S_z=0}$  as a function of distance along the armchair direction and found a smooth decrease without oscillations, again consistent with RKKY results. On the other hand, Fig. 2a shows that the magnetic

coupling between the bare vacancies is strongly affected by  $t_{nnn}$ . For  $t_{nnn} = -0.1 \text{ eV}$ , the value usually accepted for graphene systems, the oscillations lose their characteristic period of  $3a$ , where  $a = 2.46 \text{ \AA}$  is the lattice constant of graphene. Moreover, for  $t_{nnn} = -0.2 \text{ eV}$ , the ground state total spin projection becomes  $S_z = 0$ , and the staggered magnetization defined as  $(-1)^x(n_{i\downarrow} - n_{i\uparrow})/2$  where  $x$  is even for A and odd for B sublattice sites, is completely suppressed as shown in Fig. 2b. The losing of staggered magnetization is also observed for the AB configuration as shown in Fig. 2d. These results shown that magnetic properties of the double vacancy system are sensitive to  $t_{nnn}$ . In the remaining of this work,  $t_{nnn}$  will be set to zero.

#### 3.3. Mean-Field Hubbard results for charged vacancies

We now investigate the effect of the Coulomb coupling strength  $\beta$ . Figures 3a and 3c show  $E_{S_z=1} - E_{S_z=0}$  as a function of  $R/b$  for different values of  $\beta$ , for the AA and AB configurations respectively obtained using MFH calculations excluding long-range electron-electron interactions. Even at low values of  $\beta = 0.1$ ,  $S_z = 0$  becomes the ground state for AA configurations, and staggered magnetization is quenched (see Fig. 3b). A similar quenching of staggered magnetization is also observed for the AB configuration. As  $\beta$  is increased further, spin gaps gradually approach zero for both AA and AB configurations.

In order to understand the behaviour of the spin gap shown in Fig. 3 further, we plot the tight-binding energy differences between the two vacancy states as a function of  $R/b$  for different  $\beta$  values as shown in Fig. 4. Clearly, the tight-binding energy gaps show qualitatively similar features compared to the spin gaps shown in Fig. 3a and c, except for the AA configuration at  $\beta = 0$ . Indeed the vacancy states are degenerate in this latter case and the spin gap is dominated by electron-

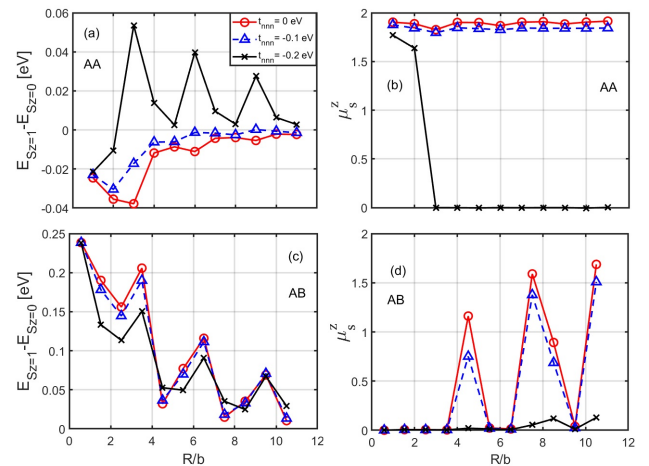


**Figure 2:** (a,c) Ground state energy differences  $E_{S_z=1} - E_{S_z=0}$  for AA and AB cases and  $\beta = 0$ , (b,d) corresponding staggered magnetisms versus  $R/b$ . Results are obtained using MFH method for hexagonal armchair GQD with 5512 atoms for different second nearest neighbor hopping parameters  $t_{nnn}$ .

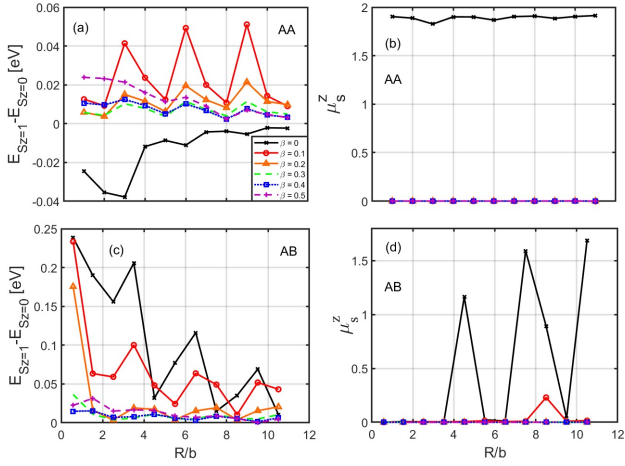


**Figure 3:** (a,c) Ground state energy differences  $E_{S_z=1} - E_{S_z=0}$  and (b,d) corresponding staggered magnetisms versus  $R/b$  for different  $\beta$  values obtained using MFH method for hexagonal armchair GQD with 5512 atoms.

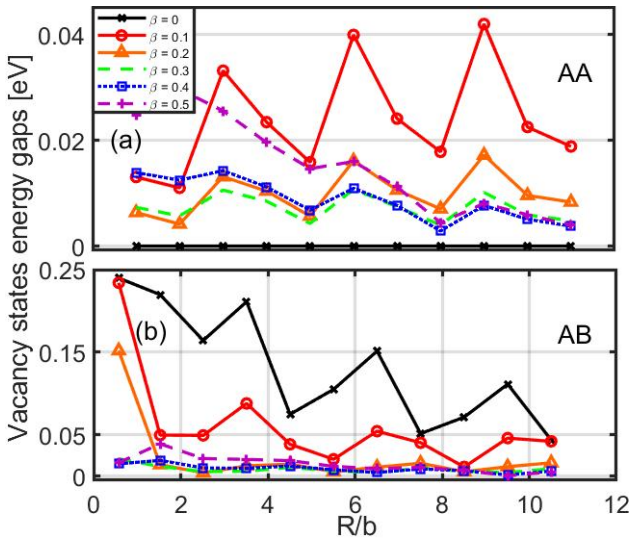


**Figure 4:** TB vacancy states gap for (a) AA and (b) AB cases along zigzag direction versus  $R/b$  for different  $\beta$  values.

electron interactions, leading to an effective ferromagnetic interaction. In other cases, the degeneracy is lifted and the spin gaps are mainly dictated by tight-binding kinetic energies.

### 3.4. Extended Mean-Field Hubbard Method calculations

We now investigate the effects of long-range electron-electron interaction terms  $V_{ij}$ . Since charged impurities causes the charge distribution to be inhomogeneous, long-range electron interactions can be expected to play an important role. Figure 5 shows the spin gaps  $E_{S_z=1} - E_{S_z=0}$  and energy spectra for for spin up electrons obtained using the extended mean-field Hubbard model. Although Figs. 5a,c are qualitatively similar to Figs. 3a,c, we see that it takes larger values of  $\beta$  to cause any change in the ground states for both AA

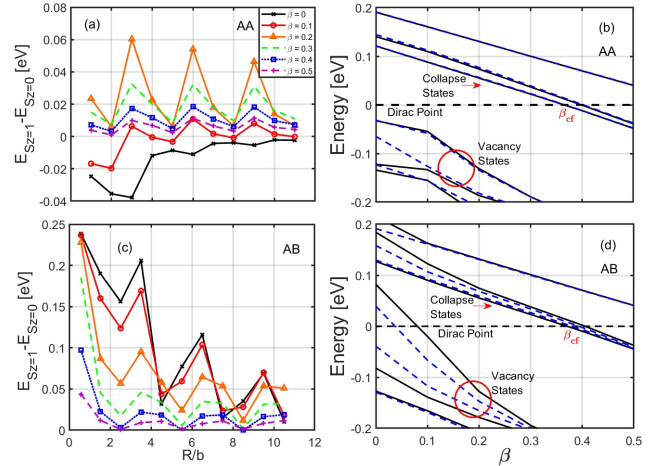


**Figure 5:** (a,c) Ground state energy differences  $E_{S_z=1} - E_{S_z=0}$  versus  $R/b$  for different  $\beta$  values, and (b,d) energy spectra versus  $\beta$  for  $R/b = 3$  (black-solid lines) and  $R/b = 9$  (blue-dashed lines). Results are obtained using extended MFH method for GQD's with 5512 atoms.

and AB configurations. In particular, for AA configuration at  $\beta = 0.1$ ,  $S_z = 1$  remains the ground state for several  $R$  values, unlike in Fig. 3a. This is due to the screening of charged impurities by electron-electron interactions. Also,  $\beta_{cf}$  value is increased to 0.36, consistent with single charged vacancy results where  $\beta_c$  is increased from 0.5 to 0.7 [51].

## 4. Summary

To conclude, we have investigated the electronic and magnetic properties of a system of two charged vacancies in hexagonal graphene quantum dots using mean-field Hubbard approach. We focused on two properties: (i) stability magnetic of phases of the two impurity system and (ii) critical value of the Coulomb potential strength for the frustrated collapse  $\beta_{cf}$ . We found that the magnetic properties are sensitive to next nearest neighbor hopping parameter  $t_{mn}$  and  $\beta$ . In particular, if  $\beta$  approaches 0.2, staggered magnetization is strongly suppressed pointing to a non-magnetic regime within the subcritical region of molecular collapse. On the other hand,  $\beta_{cf}$  is found to be nearly constant for quantum dots sizes containing more than few thousands of atoms. Finally, long range electron-electron interactions cause an increase up to 28% of  $\beta_{cf}$  as a result of smearing out the electron density near the Coulomb impurities.

## 5. ACKNOWLEDGMENT

This research was supported by the Scientific and Technological Research Council of Turkey TÜBİTAK under the 1001 grant project number 116F152, Turkey.

## References

- [1] M. M. Ugeda, I. Brihuega, F. Guinea, J. M. Gómez-Rodríguez, Missing atom as a source of carbon magnetism, *Phys. Rev. Lett.* 104 (2010) 096804. doi:10.1103/PhysRevLett.104.096804.
- [2] R. R. Nair, M. Sepioni, I.-L. Tsai, O. Lehtinen, J. Keinonen, A. V. Krasheninnikov, T. Thomson, A. K. Geim, I. V. Grigorieva, Spin-half paramagnetism in graphene induced by point defects, *Nature Physics* 8 (3) (2012) 199–202. doi:10.1038/nphys2183.
- [3] R. R. Nair, I.-L. Tsai, M. Sepioni, O. Lehtinen, J. Keinonen, A. V. Krasheninnikov, A. H. Castro Neto, M. I. Katsnelson, A. K. Geim, I. V. Grigorieva, Dual origin of defect magnetism in graphene and its reversible switching by molecular doping, *Nature Communications* 4 (1) (2013) 2010. doi:10.1038/ncomms3010.
- [4] Y. Zhang, S.-Y. Li, H. Huang, W.-T. Li, J.-B. Qiao, W.-X. Wang, L.-J. Yin, K.-K. Bai, W. Duan, L. He, Scanning tunneling microscopy of the  $\pi$  magnetism of a single carbon vacancy in graphene, *Phys. Rev. Lett.* 117 (2016) 166801. doi:10.1103/PhysRevLett.117.166801.
- [5] J. Yan, M. S. Fuhrer, Correlated charged impurity scattering in graphene, *Phys. Rev. Lett.* 107 (2011) 206601. doi:10.1103/PhysRevLett.107.206601.
- [6] Y. Wang, D. Wong, A. V. Shytov, V. W. Brar, S. Choi, Q. Wu, H.-Z. Tsai, W. Regan, A. Zettl, R. K. Kawakami, S. G. Louie, L. S. Levitov, M. F. Crommie, Observing atomic collapse resonances in artificial nuclei on graphene, *Science* 340 (6133) (2013) 734–737. doi:10.1126/science.1234320.
- [7] P. Esquinazi, A. Setzer, R. Höhne, C. Semmelhack, Y. Kopelevich, D. Spemann, T. Butz, B. Kohlstrunk, M. Lösche, Ferromagnetism in oriented graphite samples, *Phys. Rev. B* 66 (2002) 024429. doi:10.1103/PhysRevB.66.024429.
- [8] P. Esquinazi, D. Spemann, R. Höhne, A. Setzer, K.-H. Han, T. Butz, Induced magnetic ordering by proton irradiation in graphite, *Phys. Rev. Lett.* 91 (2003) 227201. doi:10.1103/PhysRevLett.91.227201.
- [9] D. C. Elias, R. R. Nair, T. M. G. Mohiuddin, S. V. Morozov, P. Blake, M. P. Halsall, A. C. Ferrari, D. W. Boukhvalov, M. I. Katsnelson, A. K. Geim, K. S. Novoselov, Control of graphene's properties by reversible hydrogenation: Evidence for graphene, *Science* 323 (5914) (2009) 610–613. doi:10.1126/science.1167130.
- [10] A. C. Neto], V. Kotov, J. Nilsson, V. Pereira, N. Peres, B. Uchoa, Adatoms in graphene, *Solid State Communications* 149 (27) (2009) 1094 – 1100, recent Progress in Graphene Studies. doi:https://doi.org/10.1016/j.ssc.2009.02.040.
- [11] K. M. McCreary, A. G. Swartz, W. Han, J. Fabian, R. K. Kawakami, Magnetic moment formation in graphene detected by scattering of pure spin currents, *Phys. Rev. Lett.* 109 (2012) 186604. doi:10.1103/PhysRevLett.109.186604.
- [12] V. M. Pereira, F. Guinea, J. M. B. Lopes dos Santos, N. M. R. Peres, A. H. Castro Neto, Disorder induced localized states in graphene, *Phys. Rev. Lett.* 96 (2006) 036801. doi:10.1103/PhysRevLett.96.036801.
- [13] F. Muñoz Rojas, J. Fernández-Rossier, J. J. Palacios, Giant magnetoresistance in ultrasmall graphene based devices, *Phys. Rev. Lett.* 102 (2009) 136810. doi:10.1103/PhysRevLett.102.136810.
- [14] A. H. Castro Neto, F. Guinea, N. M. R. Peres, K. S. Novoselov, A. K. Geim, The electronic properties of graphene, *Rev. Mod. Phys.* 81 (2009) 109–162. doi:10.1103/RevModPhys.81.109.
- [15] O. V. Yazyev, Emergence of magnetism in graphene materials and nanostructures, *Reports on Progress in Physics* 73 (5) (2010) 056501. doi:10.1088/0034-4885/73/5/056501.
- [16] E. R. Mucciolo, C. H. Lewenkopf, Disorder and electronic transport in graphene, *Journal of Physics: Condensed Matter* 22 (27) (2010) 273201. doi:10.1088/0953-8984/22/27/273201.
- [17] J. Balakrishnan, G. K. W. Koon, A. Avsar, Y. Ho, J. H. Lee, M. Jaiswal, S.-J. Baeck, J.-H. Ahn, A. Ferreira, M. A. Cazalilla, A. H. C. Neto, B. Özyilmaz, Giant spin hall effect in graphene grown by chemical vapour deposition, *Nature Communications* 5 (1) (2014) 4748. doi:10.1038/ncomms5748.
- [18] A. V. Shytov, M. I. Katsnelson, L. S. Levitov, Atomic collapse and quasi-rydberg states in graphene, *Phys. Rev. Lett.* 99 (2007) 246802. doi:10.1103/PhysRevLett.99.246802.
- [19] A. Shytov, M. Rudner, N. Gu, M. Katsnelson, L. Levitov, Atomic collapse, lorentz boosts, klein scattering, and other quantum-relativistic phenomena in graphene, *Solid State Communications* 149 (27) (2009) 1087 – 1093, recent Progress in Graphene Studies. doi:https://doi.org/10.1016/j.ssc.2009.02.043.
- [20] O. O. Sobol, E. V. Gorbar, V. P. Gusynin, Supercritical instability in graphene with two charged impurities, *Phys. Rev. B* 88 (2013) 205116. doi:10.1103/PhysRevB.88.205116.
- [21] D. Valenzuela, S. Hernández-Ortiz, M. Loewe, A. Raya, Atomic collapse in graphene: lost of unitarity, *Journal of Physics A: Mathematical and Theoretical* 49 (49) (2016) 495302. doi:10.1088/1751-8113/49/49/495302.
- [22] D. Moldovan, M. R. Masir, F. M. Peeters, Magnetic field dependence of the atomic collapse state in graphene, *2D Materials* 5 (1) (2017) 015017. doi:10.1088/2053-1583/aa9647.
- [23] J. Lu, H.-Z. Tsai, A. N. Tatan, S. Wickenburg, A. A. Omrani, D. Wong, A. Riss, E. Piatti, K. Watanabe, T. Taniguchi, A. Zettl, V. M. Pereira, M. F. Crommie, Frustrated supercritical collapse in tunable charge arrays on graphene, *Nature Communications* 10 (1) (2019) 477. doi:10.1038/s41467-019-08371-2.
- [24] V. M. Pereira, J. M. B. Lopes dos Santos, A. H. Castro Neto, Modeling disorder in graphene, *Phys. Rev. B* 77 (2008) 115109. doi:10.1103/PhysRevB.77.115109.
- [25] O. V. Yazyev, L. Helm, Defect-induced magnetism in graphene, *Phys. Rev. B* 75 (2007) 125408. doi:10.1103/PhysRevB.75.125408.
- [26] H. Sevinçli, M. Topsakal, E. Durgun, S. Ciraci, Electronic and magnetic properties of 3d transition-metal atom adsorbed graphene and graphene nanoribbons, *Phys. Rev. B* 77 (2008) 195434. doi:10.1103/PhysRevB.77.195434.
- [27] D. Soriano, N. Leconte, P. Ordejón, J.-C. Charlier, J.-J. Palacios, S. Roche, Magnetoresistance and magnetic ordering fingerprints in hydrogenated graphene, *Phys. Rev. Lett.* 107 (2011) 016602. doi:10.1103/PhysRevLett.107.016602.
- [28] A. Zhou, W. Sheng, Abnormal pseudospin-degenerate states in a graphene quantum dot with double vacancy defects, *Journal of Applied Physics* 112 (1) (2012) 014308. doi:10.1063/1.4732075.
- [29] B. S. Pujari, D. G. Kanhere, Density functional investigations of defect-induced mid-gap states in graphene, *The Journal of Physical Chemistry C* 113 (50) (2009) 21063–21067. doi:10.1021/jp907640t.
- [30] H. González-Herrero, J. M. Gómez-Rodríguez, P. Mallet, M. Moaied, J. J. Palacios, C. Salgado, M. M. Ugeda, J.-Y. Veuillen, F. Yndurain, I. Brihuega, Atomic-scale control of graphene magnetism by using hydrogen atoms, *Science* 352 (6284) (2016) 437–441. doi:10.1126/science.aad8038.
- [31] J. Mao, Y. Jiang, D. Moldovan, G. Li, K. Watanabe, T. Taniguchi, M. R. Masir, F. M. Peeters, E. Y. Andrei, Realization of a tunable artificial atom at a supercritically charged vacancy in graphene, *Nature Physics* 12 (6) (2016) 545–549. doi:10.1038/nphys3665.
- [32] I. Pomeranchuk, Y. Smorodinsky, On the energy levels of systems with  $z > 137$ , *J. Phys. USSR* (9) (1945) 97.
- [33] F. G. Werner, J. A. Wheeler, Superheavy nuclei, *Phys. Rev.* 109 (1958) 126–144. doi:10.1103/PhysRev.109.126.
- [34] W. Pieper, W. Greiner, Interior electron shells in superheavy nuclei, *Zeitschrift für Physik A Hadrons and nuclei* 218 (4) (1969) 327–340.
- [35] Y. B. Zeldovich, V. S. Popov, Electronic Structure of Superheavy Atoms, *Soviet Physics Uspekhi* 14 (6) (1972) 673–694. doi:10.1070/pu1972v014n06abeh004735.
- [36] J. Reinhardt, W. Greiner, Quantum electrodynamics of strong fields, *Reports on Progress in Physics* 40 (3) (1977) 219–295. doi:10.1088/0034-4885/40/3/001.
- [37] G. Soff, U. Mäijller, T. [de Reus], J. Reinhardt, B. Mäijller, W. Greiner, Atomic excitations in supercritical fields of giant nuclear systems, *Nuclear Instruments and Methods in Physics Research Section B: Beam Interactions with Materials and Atoms* 10-11 (1985) 214 – 218. doi:https://doi.org/10.1016/0168-583X(85)90237-X.
- [38] G. Soff, B. Müller, J. Rafelski, Precise values for critical fields in quantum electrodynamics, *Zeitschrift für Naturforschung A* 29 (9)

- (1974) 1267–1275.
- [39] V. M. Pereira, J. Nilsson, A. H. Castro Neto, Coulomb impurity problem in graphene, *Phys. Rev. Lett.* 99 (2007) 166802. doi:10.1103/PhysRevLett.99.166802.
- [40] J. Wang, M. Andjelković, G. Wang, F. M. Peeters, Molecular collapse in graphene: sublattice symmetry effect, 2020.
- [41] R. V. Pottelberge, D. Moldovan, S. P. Milovanović, F. M. Peeters, Molecular collapse in monolayer graphene, *2D Materials* 6 (4) (2019) 045047. doi:10.1088/2053-1583/ab3feb.
- [42] E. H. Lieb, Two theorems on the hubbard model, *Phys. Rev. Lett.* 62 (1989) 1201–1204. doi:10.1103/PhysRevLett.62.1201.
- [43] A. D. Güçlü, N. Bulut, Spin-spin correlations of magnetic adatoms on graphene, *Phys. Rev. B* 91 (2015) 125403. doi:10.1103/PhysRevB.91.125403.
- [44] M. Zarenia, A. Chaves, G. A. Farias, F. M. Peeters, Energy levels of triangular and hexagonal graphene quantum dots: A comparative study between the tight-binding and dirac equation approach, *Phys. Rev. B* 84 (2011) 245403. doi:10.1103/PhysRevB.84.245403.
- [45] W.-d. Sheng, M. Korkusinski, A. D. Güçlü, M. Zielinski, P. Potasz, E. S. Kadantsev, O. Voznyy, P. Hawrylak, Electronic and optical properties of semiconductor and graphene quantum dots, *Frontiers of Physics* 7 (3) (2012) 328–352. doi:10.1007/s11467-011-0200-5.
- [46] A. Altıntaş, K. E. Çakmak, A. D. Güçlü, Effects of long-range disorder and electronic interactions on the optical properties of graphene quantum dots, *Phys. Rev. B* 95 (2017) 045431. doi:10.1103/PhysRevB.95.045431.
- [47] A. Altıntaş, A. Güçlü, Defect induced anderson localization and magnetization in graphene quantum dots, *Solid State Communications* 281 (2018) 44 – 48. doi:https://doi.org/10.1016/j.ssc.2018.06.015.
- [48] A. Güçlü, K. M. Potasz, P. P. Hawrylak, *Graphene Quantum Dots*, Springer, 2014.
- [49] K. SzaĀCowski, Indirect coupling between localized magnetic moments in triangular graphene nanoflakes, *Physica E: Low-dimensional Systems and Nanostructures* 52 (2013) 46ĀĀ53. doi:10.1016/j.physe.2013.03.017.
- [50] W. L. Wang, S. Meng, E. Kaxiras, Graphene nanoflakes with large spin, *Nano Letters* 8 (1) (2008) 241–245. doi:10.1021/nl072548a.
- [51] M. Polat, H. Sevinçli, A. D. Güçlü, Collapse of the vacuum in hexagonal graphene quantum dots: A comparative study between tight-binding and mean-field hubbard models, *Phys. Rev. B* 101 (2020) 205429. doi:10.1103/PhysRevB.101.205429.
- [52] R. Van Pottelberge, M. Zarenia, P. Vasilopoulos, F. M. Peeters, Graphene quantum dot with a coulomb impurity: Subcritical and supercritical regime, *Phys. Rev. B* 95 (2017) 245410. doi:10.1103/PhysRevB.95.245410.
- [53] A. V. Shytov, M. I. Katsnelson, L. S. Levitov, Vacuum polarization and screening of supercritical impurities in graphene, *Phys. Rev. Lett.* 99 (2007) 236801. doi:10.1103/PhysRevLett.99.236801.
- [54] V. N. Kotov, B. Uchoa, V. M. Pereira, F. Guinea, A. H. Castro Neto, Electron-electron interactions in graphene: Current status and perspectives, *Rev. Mod. Phys.* 84 (2012) 1067–1125. doi:10.1103/RevModPhys.84.1067.
- [55] T. Ando, Screening effect and impurity scattering in monolayer graphene, *Journal of the Physical Society of Japan* 75 (7) (2006) 074716. doi:10.1143/JPSJ.75.074716.
- [56] P. Potasz, A. D. Güçlü, P. Hawrylak, Spin and electronic correlations in gated graphene quantum rings, *Phys. Rev. B* 82 (2010) 075425. doi:10.1103/PhysRevB.82.075425.
- [57] A. M. Black-Schaffer, Rkky coupling in graphene, *Phys. Rev. B* 81 (2010) 205416. doi:10.1103/PhysRevB.81.205416.